

Electronic Spectroscopy of Monocyclic Carbon Ring Cations for Astrochemical Consideration

Published as part of *The Journal of Physical Chemistry virtual special issue "10 Years of the ACS PHYS Astrochemistry Subdivision"*.

Johanna Rademacher, Elliott S. Reedy, and Ewen K. Campbell*

Cite This: *J. Phys. Chem. A* 2022, 126, 2127–2133

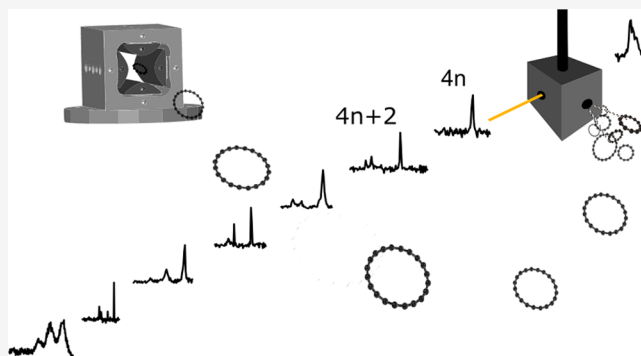
Read Online

ACCESS |

Metrics & More

Article Recommendations

ABSTRACT: Gas phase electronic spectra of pure carbon cations generated by laser vaporization of graphite in a supersonic jet and cooled to below 10 K and tagged with helium atoms in a cryogenic trap are presented. The measured C_{2n}^+-He with n from 6 to 14, are believed to be monocyclic ring structures and possess an origin band wavelength that shifts linearly with the number of carbon atoms, as recently demonstrated through N_2 tagging by Buntine et al. (*J. Chem. Phys.* 2021, 155, 214302). The set of data presented here further constrains the spectral characteristics inferred for the bare C_{2n}^+ ions to facilitate astronomical searches for them in diffuse clouds by absorption spectroscopy.



INTRODUCTION

Since the detection of long polar chains in dense clouds in the 1970s,^{1–4} carbon containing molecules have played an important role in astrochemical studies. In contemporary work, the first carbon ring structures were identified by rotational spectroscopy; cyanobenzene, $c-C_6H_5CN$,⁵ and 1- and 2-cyanonaphthalene, $C_{10}H_7CN$.⁶ These possess large dipole moments so can be observed by radiotelescopes, and their detection is of relevance to the PAH hypothesis and thus the quest to reveal the nature of the species responsible from the so-called unidentified infrared bands (UIR) bands.⁷

Pure carbon structures are not amenable to detection by such methods, but they can be searched for based on their electronic transitions in absorption. This approach has been used to detect the spectroscopic fingerprints of the Buckminsterfullerene cation, C_{60}^+ , in diffuse clouds.^{8,9} This soccer ball is the only identified species found to be responsible for a handful of diffuse interstellar bands (DIBs)^{10–13} and is remarkably abundant in these environments,¹⁴ presumably due to its resilience against destruction.

Other carbon isomers are also of interest in relation to the DIB enigma, but a lack of spectroscopic data has prevented evaluation of their astrochemical importance. This statement is particularly relevant for other open-shell C_n^+ cations¹⁵ which, due to their low ionization potentials,¹⁶ may be expected to be prevalent as for C_{60}^+ in environments bathed in photons with energies up to 13.6 eV. The versatile bonding of carbon leads

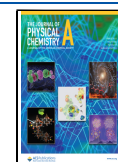
to a variety of ionic structures ranging from linear chains to mono- and bicyclic rings and fullerenes, as revealed in ion mobility studies.^{17–19} The detection of their absorptions under appropriate conditions to enable comparison with astronomical data is an experimental challenge. As a result, little spectroscopic data has been added to that compiled in the reviews in the 1990s by van Orden and Saykally,²⁰ and Bowers and colleagues,¹⁸ in which this knowledge gap was highlighted. To address this, approaches involving nonstandard methods for synthesis combined with cooling, and action spectroscopy in cryogenic traps have been recently applied.²¹

An instrument was constructed in our laboratory to combine laser vaporization synthesis with mass-selection and cryogenic ion trapping spectroscopy, and proof-of-principle results on helium tagged cyclic C_6^+ were presented.²² Various action spectroscopy methods were used to detect the ${}^2\Pi_g \leftarrow X {}^2\Sigma_u^+$ electronic transition of linear C_5^+ .²³ In the latter study, spectra of $C_5^+-He_n$ ($n = 1–3$) were used to predict the absorption wavelengths for the bare ion. This was proved by more direct 2-color experiments that monitored fragmentation of C_5^+ into

Received: January 26, 2022

Revised: March 11, 2022

Published: March 28, 2022



$C_3^+ + C_2$. Interestingly, a blue shift in the absorption wavelengths with n was observed, with a helium atom shifting the absorption bands of C_5^+ by around 10 cm^{-1} . The same apparatus was used to spectroscopically show that the soccer ball isomer is the dominant structure with $m/z = 720$ produced by laser vaporization in the ion source.²⁴

Buntine et al. very recently presented results using an instrument that combines ion mobility with spectroscopic characterization in a cylindrical ion trap at 25 K, reporting N_2 tagged data of C_{2n}^+ monocyclic rings, with $n = 6-14$. These beautiful experiments are a breakthrough in attempts to attain the electronic spectra of carbon cations and reveal that the lowest energy doublet electronic transitions shift linearly to longer wavelengths with increasing n .²⁵ The behavior thus resembles that observed for linear chains by Maier and colleagues, with examples being C_n and the neutral and positively charged polyacetylenes HC_nH .²⁶

Concerning the geometrical and electronic structure of cationic monocyclic rings, the only computational studies reported have used density functional theory (DFT) approaches.^{27,28} As noted elsewhere, such methods can be unreliable even for neutral carbon ring structures, leading to incorrect predictions of cumulenic/polyynic bonding.^{29,30} Recent studies suggest that a careful choice of functionals might be able to circumvent these problems and make DFT applicable to similar systems in the future.^{31,32} The open-shell nature of the C_{2n}^+ considered in the present study, however, require theoretical work using multireferential methods, but unfortunately no high level computations are currently available for these systems.

The C_{2n}^+ ($n = 6-14$) species reported in ref 25 are of interest in the context of the DIBs because their wavelength range (400–1400 nm) spans the region where the majority of them are found. The measured bandwidths show an alteration with $2n$, and the narrowest absorptions have widths of $10-20\text{ cm}^{-1}$ in the visible, making them appealing targets for further laboratory and observational studies. In this contribution, the electronic spectra of helium tagged C_{2n}^+ ($n = 6-14$) are reported. These data are expected to be less perturbed by the tag and are reported to better constrain astronomical searches for these pure carbon structures.

EXPERIMENTAL SECTION

Experiments were carried out using a recently constructed instrument described in detail in ref 22. Briefly, pulsed $\lambda = 355\text{ nm}$ radiation (20 mJ/pulse) was focused onto a rotating and translating graphite rod producing C_{2n}^+ that were expanded in a supersonic jet of helium. After collimation with a skimmer, ions were transmitted through a quadrupole mass filter and turned through 90° before loading into the linear quadrupole ion trap, operating at a nominal (trap wall) temperature, $T_{\text{nom}} = 4-5\text{ K}$. Several pulses of ions, produced at 10 Hz , were accumulated in the trap and cooled through collisions with helium buffer gas, for several hundred milliseconds. Under these conditions, it was possible to convert a proportion of C_{2n}^+ into $C_{2n}^+-\text{He}$ complexes. After pumping out the buffer gas, the trap contents were analyzed using a quadrupole mass-spectrometer coupled to a Daly detector.

Photofragmentation spectra were collected by exposing the stored ions to radiation from a pulsed, tunable OPO system supplying radiation over the $470-1340\text{ nm}$ range with a bandwidth of 5 cm^{-1} . The OPO wavelength was calibrated

using a wavemeter. Spectra were acquired with a step size of $0.1-0.4\text{ nm}$ at shorter wavelengths than 700 nm . At longer wavelengths, the minimum step size of 1 nm was used. On resonance with an electronic transition of $C_{2n}^+-\text{He}$, this led to dissociation of the complex by loss of the helium atom. To account for fluctuations in the number of stored ions, data were collected on alternate trapping cycles (repeated at 1 Hz) with (N_i) and without (N_0) exposure to the OPO, which was controlled by use of a mechanical shutter. By monitoring the attenuation ($1 - N_i/N_0$), $C_{2n}^+-\text{He}$ photofragmentation spectra were obtained. The power of the OPO system was attenuated such that less than 30% of the $C_{2n}^+-\text{He}$ were dissociated. The presented spectra are corrected for changes to the OPO power as a function of wavelength and are reported in air.

RESULTS AND DISCUSSION

Electronic Spectra. The electronic spectra of $C_{2n}^+-\text{He}$ ($n = 6-14$) complexes are presented in Figure 1, showing a

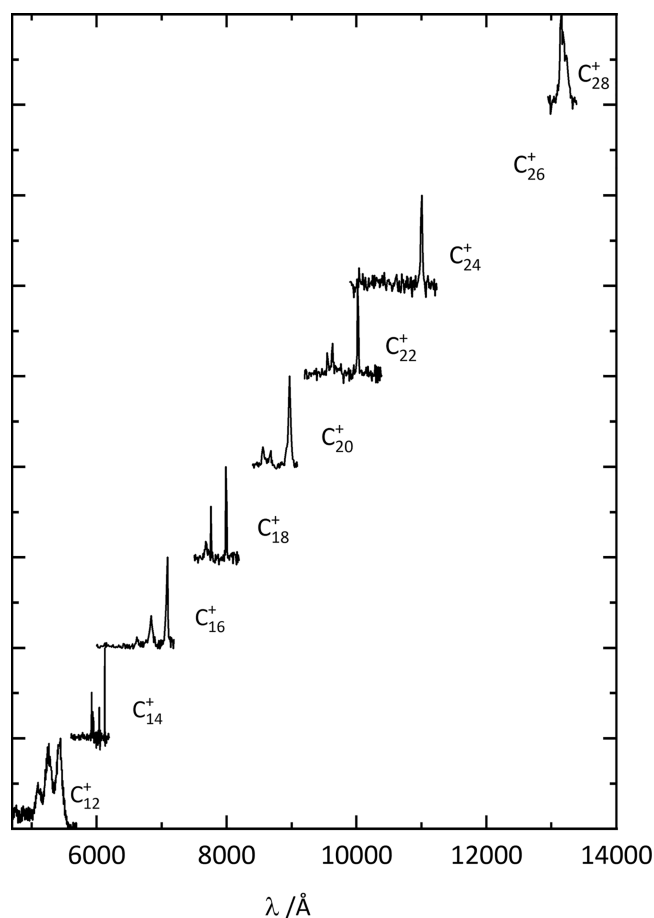


Figure 1. Electronic spectra of $C_{2n}^+-\text{He}$ observed by monitoring the wavelength dependent loss of the helium atom. The data are believed to be the lowest energy doublet transitions of monocyclic cation ring structures.

linear increase in the wavelength of the origin bands with increasing ring size. A similar result for $C_{2n}^+-N_2$ has been reported in ref 25 and provides confidence that the same molecular structures are probed in both experiments. The observed spectra are believed to be the lowest energy doublet

electronic transitions of these open-shell carbon cations, and in most cases, the pattern is dominated by a strong origin band.

The assignment of these spectra to a series of monocyclic rings possessing similar structures suggests that information on the isomeric composition of C_{2n}^+ produced in the source can be obtained. To investigate this, the stored C_{2n}^+ -He ions were irradiated with high fluence at the wavelength of their absorption bands shown in Figure 1. These experiments led to a maximum attenuation, and from this the number of C_{2n}^+ -He remaining in the trap and having a different geometric structure can be estimated. The results of these attenuation experiments are listed in Table 1.

Table 1. Observed Maximum Attenuation ($1 - \frac{N_i}{N_0}$) of

C_n^+ -He Complexes Following Irradiation at the Wavelength of Their Band Maxima Using High Fluence

C_n^+ -He		$1 - \frac{N_i}{N_0}$
n	irradiation wavelength/Å	
12	5439	0.97 ± 0.02
14	6123	0.96 ± 0.03
16	7088	0.97 ± 0.01
18	7988	0.93 ± 0.02
20	8968	0.96 ± 0.02
22	10017	0.67 ± 0.10
24	11007	0.60 ± 0.07
26		
28	13156	0.27 ± 0.14

Previous ion mobility experiments revealed that in the size range containing between 10 and 20 carbon atoms, cations with monocyclic ring structures are almost exclusively produced by laser vaporization of graphite.¹⁸ This is broadly consistent with the values presented in Table 1, based on spectroscopic measurement. For larger species, C_{22}^+ - C_{28}^+ , the number of complexes that do not interact with the radiation increases from about 30% for C_{22}^+ to ~70% at C_{28}^+ . Ion mobility studies indicate a significant reduction in % of monocycles should be expected in this region, where bicyclic structures become increasingly important. Note, however, that the number of C_{2n}^+ monocycles in the range $n = 11$ -14 inferred in the present work diverges somewhat from the values presented in ref 18, where 50% of C_{28}^+ possess the same monocyclic ring structure. The differences between ion mobility and these spectroscopic results may be due to several reasons. For example, it is important to note that in the present work, the experiment is sensitive to the percentages of helium complexes depleted, which may not necessarily reflect the ratios of parent untagged C_{2n}^+ synthesized in the source. Different binding energies of the helium atoms for other structures, or relaxation processes that do not lead to the loss of the helium atom, could distort the isomeric picture inferred. Another possibility is that the conditions in the ions source (λ , fluence, pulse length/intensity) influence the distribution in this size range.

The wavelengths of the origin bands of the C_{2n}^+ -He electronic transitions assigned to monocyclic rings are plotted in Figure 2, and they are also listed in Table 2. The profiles of the C_{2n}^+ -He absorptions are asymmetric; therefore, band maxima are listed rather than the results of fits. The large step

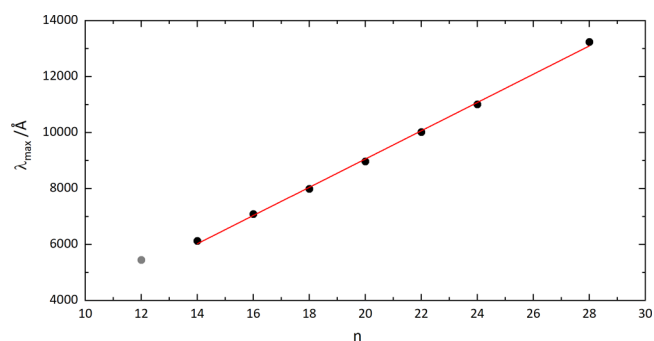


Figure 2. Wavelengths of origin band maxima as a function the number of carbon atoms (black). A linear fit to these wavelengths is the red line.

Table 2. Origin Band Maxima and fwhm's for the Observed C_n^+ -He Cations

C_n^+ -He			C_n^{+c}
n	$\lambda_{\max}^a/\text{Å}$	fwhm/Å	$\lambda_{\max}/\text{Å}$
12	5424 ± 10	76	5425 ± 10
14	6124 ± 1	2-3	6126 ± 2
16 ^b	7086 ± 5	27	7088 ± 5
18	7991 ± 5	17	7995 ± 6
20	8968 ± 5	39	8972 ± 6
22	10020 ± 5	20	10025 ± 6
24	11005 ± 5	32	11012 ± 9
26			
28	13234 ± 7	60	13243 ± 10

^aReported uncertainties are $\pm \frac{1}{2}$ the OPO bandwidth for C_{14}^+ , and $\pm \frac{1}{2}$ the step size for C_{16}^+ to C_{24}^+ . The C_{12}^+ and C_{28}^+ characteristics are from Lorentzian fits to the observed data. ^bUncertain due to change from the signal to the idler at 710 nm. ^cPredicted wavelengths for the untagged C_n^+ ions are based on extrapolation of C_n^+ -He_{1,2} data shown in Figure 5 for C_{14}^+ and C_{24}^+ . For the other C_n^+ ions, the average value of 5 cm⁻¹ was used (see text for details).

size in wavelength of the OPO coupled with the width/appearance of the narrowest features indicates that the origin band maxima are likely to fall between data points, particularly for the C_{4n+2}^+ spectra. The band maxima reported in Table 2 were estimated using the weighted average of the intensity of the data points closest to the one showing the strongest attenuation. For example, for C_{18}^+ -He, the weighted average of three points gives 7991 Å compared with the data point at maximum intensity, 7988 Å. In comparison with the C_{2n}^+ -N₂ data reported in ref 25, the C_{4n+2}^+ -He absorptions lie to the red and are shifted by between 3 and 26 cm⁻¹. Both blue and red shifts are observed for the C_{4n}^+ -He in comparison to the values listed in Table 1 of ref 25. Note also that the N₂ tagged data were obtained at a higher trap temperature (25 K) than in the present work.

To compare the electronic spectra of the C_{2n}^+ -He rings, they are plotted in Figure 3. A general trend reported in ref 25 is that the $4n + 2$ monocyclic cations show narrower (fwhm ≈ 10 -20 cm⁻¹) absorptions than the $4n$ series (fwhm > 100 cm⁻¹). These two groups are expected to differ in terms of their aromatic/antiaromatic nature. Buntine et al. suggest a possible reason for the narrow/broad fwhm variation of the C_{4n+2}^+/C_{4n}^+ series with reference to the DFT calculations reported by Giuffreda et al.²⁷ In particular, it was noted that a quartet excited state lies just above the doublet ground

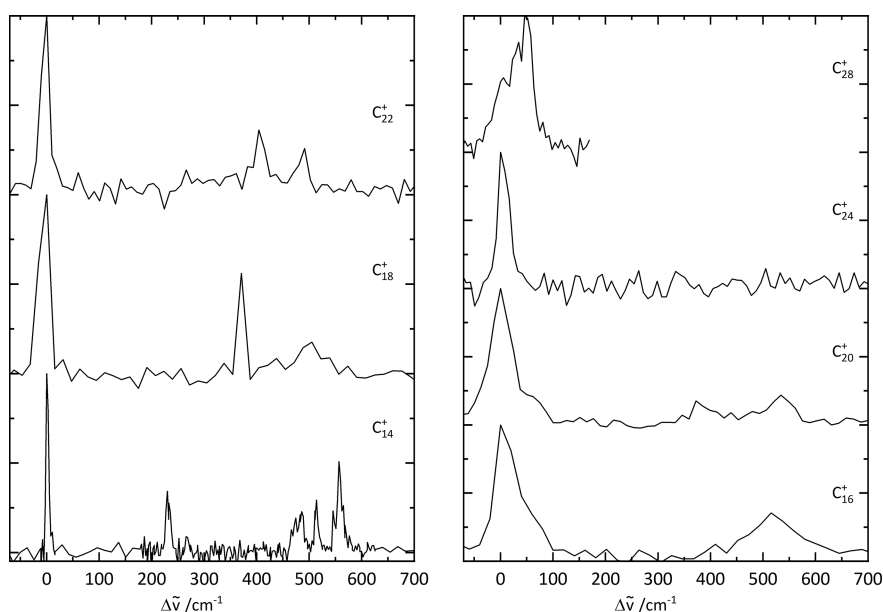


Figure 3. Electronic spectra of monocyclic cations plotted as a function of energy $\Delta\bar{\nu}$ from the origin band. The data are separated into $4n + 2$ (left) and $4n$ (right) series.

electronic state for the C_{4n}^+ ions but higher in energy for the C_{4n+2}^+ series. Thus, it was suggested that the electronically excited C_{4n}^+ may decay through rapid intersystem crossing due to the high density of quartet vibronic states iso-energetic with the photoexcited doublet, leading to broader widths.²⁵

These trends are broadly reflected in the helium tagged C_{2n}^+ spectra; however, the distinction between C_{4n+2}^+ and C_{4n}^+ in terms of width becomes less clear-cut as n increases. The fwhm values reported here are determined directly from the measured $C_{2n}^+ - \text{He}$ data and should be considered as upper limits for the narrower origin bands (e.g., C_{14}^+ , C_{18}^+ , C_{22}^+) due to the OPO wavelength step size. The width of the origin band of C_{14}^+ of around 6 cm^{-1} would correspond to an excited state lifetime of $\sim 0.9 \text{ ps}$. The other $4n + 2$ species observed in the present study, C_{18}^+ and C_{22}^+ , have origin bands that are a bit broader and possess similar fwhm's of around 25 cm^{-1} . Interestingly, despite the ability to produce $C_{26}^+ - \text{He}$, the monocyclic ring isomer could not be spectroscopically detected, even with the accurate prediction of its origin band wavelength based on Figure 2. This is surprising and based on Table 1, unlikely to be due to a lack of monocyclic cation isomers with $m/z = 312$. Rather, it is speculated that changes to the electronic structure and excited state decay mechanisms at this size may be responsible.

On the other hand, the spectra of helium tagged C_{4n}^+ rings show some trends. In particular, the fwhm of their origin bands decreases with increasing ring size, with C_{12}^+ being (by far) the broadest. The fwhm's for C_{12}^+ , C_{16}^+ , C_{20}^+ , C_{24}^+ are 258, 53, 50, 26 cm^{-1} , respectively. A decrease in the width of the origin bands with increasing size may be anticipated based on their decreasing rotational constants. However, the fwhm's obtained in the present study are broader than expected for the extent of the rotational envelope in doublet–doublet transitions of monocyclic rings of this size range ($\sim 2\text{--}6 \text{ cm}^{-1}$ at 10 K) and are likely to reflect lifetime effects to a greater extent. The shapes of the origin bands in both C_{4n}^+ and C_{4n+2}^+ spectra are asymmetric and not well reproduced by a single Lorentzian function.

The lowest energy portion of the of $C_{28}^+ - \text{He}$ spectrum is shown in Figure 4. The appearance differs somewhat from that

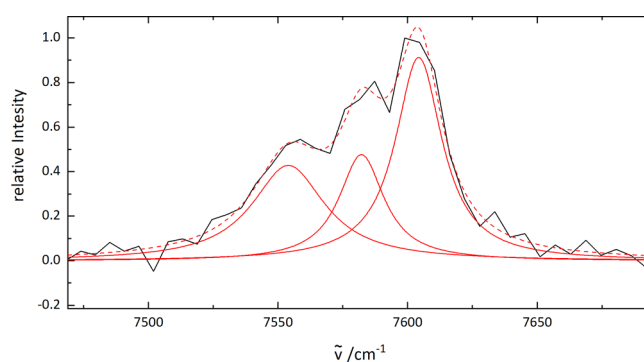


Figure 4. Lowest energy portion of the $C_{28}^+ - \text{He}$ spectrum. The profile suggests more than one unresolved component and has been fit with three Lorentzian functions (red); the cumulative result is the dotted line.

of the other $4n$ cations and a fit to the profile suggest the presence of three unresolved features separated by $\sim 25 \text{ cm}^{-1}$. Due to the rather low abundance of monocyclic structures tagged with helium ($m/z = 340$), the measured data may show some additional broadening due to saturation. Nevertheless, separation of the envelope into three contributions as shown in Figure 4, suggests a fwhm for the origin of $\sim 34 \text{ cm}^{-1}$ which is more consistent with the values for the other $4n$ species. These absorptions could arise due to excitation of a low-frequency vibrational mode of C_{28}^+ in the excited electronic state or of a mode involving the weakly bound helium atom. It is speculated that the latter explanation, arising from a change in the $C_{28}^+ \cdots \text{He}$ interaction potential between the ground and excited states may be less likely, as no such patterns are found in the other helium tagged C_{2n}^+ spectra. In ref 25 (Supporting Information), harmonic frequencies of C_{20}^+ were reported, including the mode $\nu_{54} = 21 \text{ cm}^{-1}$ so it is conceivable that a

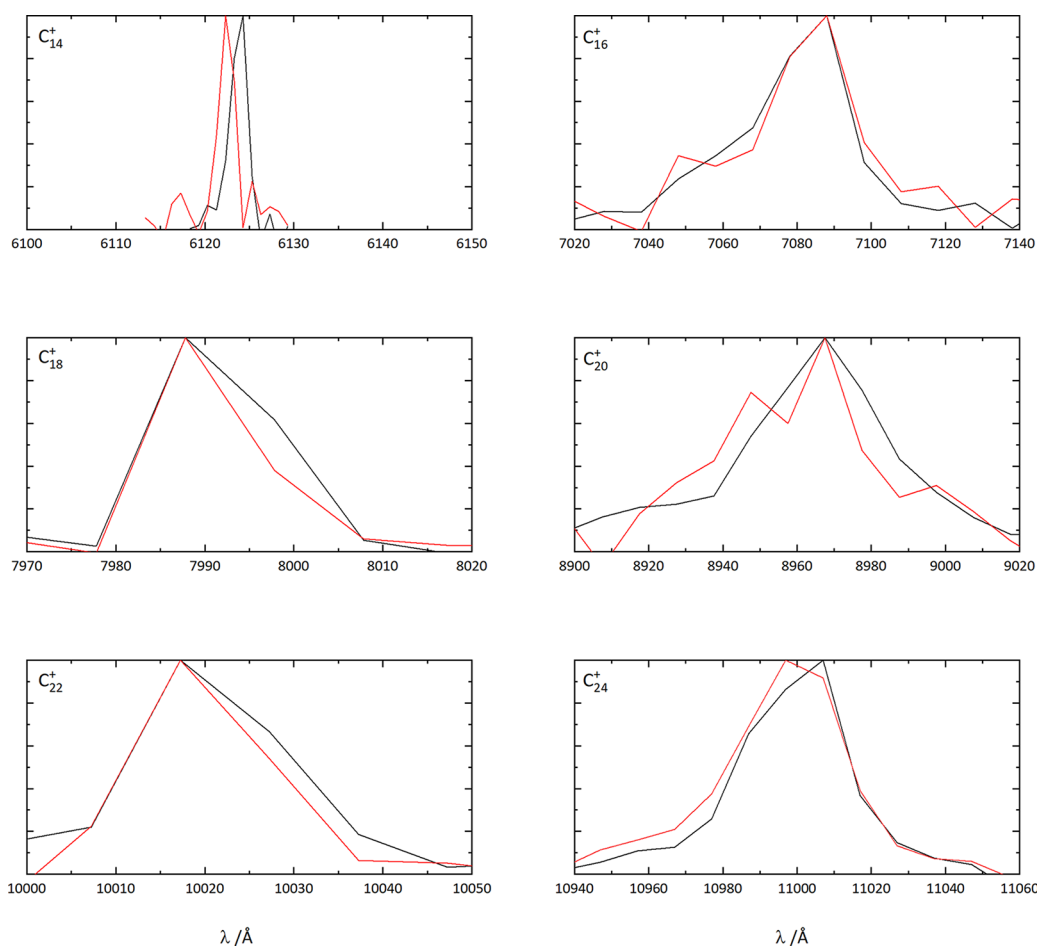


Figure 5. Electronic spectra of monocyclic cations tagged with one (black) and two (red) helium atoms. The data are separated into $4n + 2$ (left) and $4n$ (right) series.

low frequency ring vibration in the C_{28}^+ excited state is responsible for the pattern.

On Comparisons with Astronomical Observations. The electronic spectra of monocyclic rings C_{2n}^+ ($n = 6-14$) are appealing in terms of potential astronomical detectability for a couple of reasons. First, these (presumably) lowest energy doublet transitions occur in the spectral region containing the majority of DIBs. Second, these low temperature gas phase measurements show that their electronic oscillator strengths are mostly localized in their origin bands, with the remainder contained within only a few, weaker features. This resembles the situation found for the electronic transitions of C_{60}^+ in the near-infrared and contrasts with that of C_{70}^+ . In the case of the C_{70}^+ transition around 7959 Å, the electronic band oscillator strength is distributed over tens of absorptions of similar intensity and thus each band lies below the astronomical detection limits even for column densities of 10^{13} cm^{-2} .¹⁴

The widths of the absorptions are also important to consider. The C_{4n+2}^+ species have fwhm of 20 Å or below. The narrowest is for $C_{14}^+-\text{He}$, with a fwhm of less than 3 Å near 6124 Å, which should be observable with current échelle spectrographs. Observation of DIBs broader than 6 Å presents challenges using such instrumentation, as discussed in detail in ref 33, where a number of broad DIBs are also listed. Therefore, dedicated searches based on accurate wavelengths are desirable for the other C_{4n+2}^+ and C_{4n}^+ ions.

The absorption wavelengths of the $C_{2n}^+-\text{He}$ cations presented here will be offset relative to the bare ions due to the presence of the weakly bound atom. For example, in the case of C_{60}^+ , this was determined to be less than 1 Å. For smaller carbon cations such as linear C_5^+ , it was much larger, ~ 2.7 Å at 5137 Å corresponding to around 10 cm^{-1} . Thus, one may anticipate a shift, depending on the size, of below this value. To gain some insight into this, electronic spectra of $C_{2n}^+-\text{He}_2$ were also acquired and are compared with those of $C_{2n}^+-\text{He}$ in Figure 5. This indicates a small blue shift of the $C_{2n}^+-\text{He}_2$ absorptions relative to $C_{2n}^+-\text{He}$. The wavelengths for C_{2n}^+ are thus expected to lie to the red of $C_{2n}^+-\text{He}$ by less than 6 cm^{-1} , and the predicted values for C_{2n}^+ are listed in Table 2. The offset applied is determined from the data shown in Figure 5 for C_{14}^+ and C_{24}^+ . For the other ions the predicted wavelengths are based on the average (5 cm^{-1}) of the He shift for C_{14}^+ (4 cm^{-1}) and C_{24}^+ (6 cm^{-1}). A possible exception to this trend is C_{16}^+ , where a slight red shift may be indicated between $C_{16}^+-\text{He}$ and $C_{16}^+-\text{He}_2$ data in Figure 5. However, it is difficult to make conclusive statements in this case due to a change from the signal to the idler of the used radiation source at 710 nm. The N_2 tagged spectra reported in Table 1 of ref 25 also indicate a red shift between N_2 and $(N_2)_2$ using a similar OPO. For more accurate predictions of the narrower bands, higher resolution data are required.

The proximity of the origin band wavelength of C_{14}^+ to DIBs in the visible has been noted in ref 25. The value inferred for

the bare ion based on $C_{14}^+ - (N_2)_{1,2}$ data is 6128 Å, which lies close to the 6126 ± 2 Å predicted here based on helium tagged spectra. The nearby DIB at 6128.20 Å has a fwhm of 2.18 Å,³⁴ similar to the width observed for $C_{14}^+ - He$. With reference to other nonpolar species present in the diffuse ISM (such as C_3^{35} and H_3^{+36}), the monocyclic C_{2n}^+ rings may be expected to have rotational temperatures 50–80 K, which is significantly higher than these laboratory measurements. Given the asymmetric profiles of the $C_{2n}^+ - He$ absorption bands, it would be desirable to obtain more direct measurement of the narrowest C_{2n}^+ absorptions through other action spectroscopy methods as recently demonstrated on C_5^+ ,²³ at elevated temperatures.

CONCLUSIONS

The spectra of C_{2n}^+ ($n = 6-14$) are interesting candidates for astrochemical consideration. Their electronic transitions are dominated by strong origin bands and several possess widths below 20 Å in the spectral range of interest for the DIBs. The wavelengths of the C_{2n}^+ bands predicted in the present study should guide astronomical searches in the visible/near-infrared. Conclusive assessment of the abundance of these monocyclic ring cations will, however, require a combination of both further laboratory and dedicated observational studies. Laboratory spectra recorded at higher resolution, and exploiting other action spectroscopy methods, are desirable to test the predictions of the C_{2n}^+ gas phase wavelengths on the basis of helium extrapolation. Finally, measurement of absorption cross sections or theoretical determination of accurate oscillator strengths, in combination with observational data, is a priority to enable assessment of their abundance in diffuse clouds and thus address the lack of information on the distribution of carbon cation isomers in interstellar environments.

AUTHOR INFORMATION

Corresponding Author

Ewen K. Campbell – School of Chemistry, University of Edinburgh, Edinburgh EH8 9YL, United Kingdom;
orcid.org/0000-0003-0719-0823; Phone: +44 (0)131 651 7152; Email: e.k.campbell@ed.ac.uk

Authors

Johanna Rademacher – School of Chemistry, University of Edinburgh, Edinburgh EH8 9YL, United Kingdom
Elliott S. Reedy – School of Chemistry, University of Edinburgh, Edinburgh EH8 9YL, United Kingdom

Complete contact information is available at:
<https://pubs.acs.org/10.1021/acs.jpca.2c00650>

Notes

The authors declare no competing financial interest.

ACKNOWLEDGMENTS

E.K.C. acknowledges financial assistance from the Royal Society (Grants RGF/EA/181035 and URF/R1/180162) and the School of Chemistry, University of Edinburgh.

REFERENCES

- Turner, B. E. Detection of interstellar cyanoacetylene. *Astrophys. J. Lett.* **1971**, *163*, L35–L39.
- Kroto, H. W.; Kirby, C.; Walton, D. R. M.; Avery, L. W.; Broten, N. W.; MacLeod, J. M.; Oka, T. The detection of cyanoacetylene, $H(C\equiv C)_3CN$, in Heiles's cloud 2. *Astrophys. J. Lett.* **1978**, *219*, L133–L137.
- Broten, N. W.; Oka, T.; Avery, L. W.; MacLeod, J. M.; Kroto, H. W. The detection of HC_9N in interstellar space. *ApJ. Lett.* **1978**, *223*, L105–L107.
- Winnewisser, G.; Walmsley, C. M. The detection of HC_5N and HC_7N in IRC + 10216. *Astron. Astrophys.* **1978**, *70*, L37–L39.
- McGuire, B. A.; Burkhardt, A. M.; Kalenskii, S.; Shingledecker, C. N.; Remijan, A. J.; Herbst, E.; McCarthy, M. C. Detection of the aromatic molecule benzonitrile ($c-C_6H_5CN$) in the interstellar medium. *Science* **2018**, *359*, 202–205.
- McGuire, B. A.; Loomis, R. A.; Burkhardt, A. M.; Lee, K. L. K.; Shingledecker, C. N.; Charnley, S. B.; Cooke, I. R.; Cordiner, M. A.; Herbst, E.; Kalenskii, S.; et al. Detection of two interstellar polycyclic aromatic hydrocarbons via spectral matched filtering. *Science* **2021**, *371*, 1265–1269.
- McCarthy, M. C.; McGuire, B. A. Aromatics and cyclic molecules in molecular clouds: a new dimension of interstellar organic chemistry. *J. Phys. Chem. A* **2021**, *125*, 3231–3243.
- Foing, B. H.; Ehrenfreund, P. Detection of two interstellar absorption bands coincident with spectral features of C_{60}^+ . *Nature* **1994**, *369*, 296–298.
- Foing, B. H.; Ehrenfreund, P. New evidences for interstellar C_{60}^+ . *Astron. Astrophys.* **1997**, *317*, L59–L62.
- Campbell, E. K.; Holz, M.; Gerlich, D.; Maier, J. P. Laboratory confirmation of C_{60}^+ as the carrier of two diffuse interstellar bands. *Nature* **2015**, *523*, 322–323.
- Walker, G. A. H.; Bohlender, D. A.; Maier, J. P.; Campbell, E. K. Identification of more interstellar C_{60}^+ bands. *Astrophys. J. Lett.* **2015**, *812*, L8.
- Walker, G. A. H.; Campbell, E. K.; Maier, J. P.; Bohlender, D.; Malo, L. Gas-phase absorptions of C_{60}^+ : a new comparison with astronomical measurements. *Astrophys. J.* **2016**, *831*, 130.
- Cordiner, M. A.; Linnartz, H.; Cox, N. L. J.; Cami, J.; Najarro, F.; Proffitt, C. R.; Lallement, R.; Ehrenfreund, P.; Foing, B. H.; Gull, T. R.; Sarre, P. J.; Charnley, S. B. Confirming interstellar C_{60}^+ using the Hubble Space Telescope. *Astrophys. J. Lett.* **2019**, *875*, L28.
- Campbell, E. K.; Holz, M.; Maier, J. P.; Gerlich, D.; Walker, G. A. H.; Bohlender, D. A. Gas phase absorption spectroscopy of C_{60}^+ and C_{70}^+ in a cryogenic ion trap: comparison with astronomical measurements. *Astrophys. J.* **2016**, *822*, 17.
- Campbell, E. K.; Maier, J. P. Perspective: C_{60}^+ and laboratory spectroscopy related to diffuse interstellar bands. *J. Chem. Phys.* **2017**, *146*, 160901.
- Belau, L.; Wheeler, S. E.; Ticknor, B. W.; Ahmed, M.; Leone, S. R.; Allen, W. D.; Schaefer, H. F.; Duncan, M. A. Ionization thresholds of small carbon clusters: tunable VUV experiments and theory. *J. Am. Chem. Soc.* **2007**, *129*, 10229–10243.
- von Helden, G.; Hsu, M.-T.; Kemper, P. R.; Bowers, M. T. Structures of carbon cluster ions from 3 to 60 atoms: linears to rings to fullerenes. *J. Chem. Phys.* **1991**, *95*, 3835–3837.
- von Helden, G.; Hsu, M.-T.; Gotts, N.; Bowers, M. T. Carbon cluster cations with up to 84 atoms: structures, formation mechanism, and reactivity. *J. Phys. Chem.* **1993**, *97*, 8182–8192.
- Gotts, N. G.; von Helden, G.; Bowers, M. T. Carbon cluster anions: structure and growth from C_5^- to C_{62}^- . *Int. J. Mass Spectrom. Ion Processes* **1995**, *149-150*, 217–229.
- Van Orden, A.; Saykally, R. J. Small carbon clusters: spectroscopy, structure, and energetics. *Chem. Rev.* **1998**, *98*, 2313–2357.
- Campbell, E. K. Spectroscopy of astrophysically relevant ions in traps. *Mol. Phys.* **2020**, *118*, No. e1797918.
- Campbell, E. K.; Dunk, P. W. LV-DIB-s4PT: A new tool for astrochemistry. *Rev. Sci. Instrum.* **2019**, *90*, 103101.
- Reedy, E. S.; Rademacher, J.; Szabla, R.; Campbell, E. K. Electronic absorptions of C_5^+ detected in the visible through action spectroscopy in a cryogenic trap. *Mol. Phys.* **2022**, *120*, No. e1989070.

- (24) Campbell, E. K.; Rademacher, J.; Bana, S. M. M. Synthesis and spectroscopy of Buckminsterfullerene cation C_{60}^+ in a cryogenic ion trapping instrument. *Crystals* **2021**, *11*, 1119.
- (25) Buntine, J. T.; Cotter, M. I.; Jacovella, U.; Liu, C.; Watkins, P.; Carrascosa, E.; Bull, J. N.; Weston, L.; Muller, G.; Scholz, M. S.; et al. Electronic spectra of positively charged carbon clusters – C_{2n}^+ ($n = 6 - 14$). *J. Chem. Phys.* **2021**, *155*, 214302.
- (26) Nagarajan, R.; Maier, J. P. Electronic spectra of carbon chains and derivatives. *Int. Rev. Phys. Chem.* **2010**, *29*, 521–554.
- (27) Giuffreda, M. G.; Deleuze, M. S.; François, J. P. Structural, rotational, vibrational, and electronic properties of ionized carbon clusters C_n^+ ($n = 4 - 19$). *J. Phys. Chem. A* **1999**, *103*, 5137–5151.
- (28) Strelnikov, D. V.; Link, M.; Weippert, J.; Kappes, M. M. Optical spectroscopy of small carbon clusters from electron-impact fragmentation and ionization of fullerene- C_{60} . *J. Phys. Chem. A* **2019**, *123*, 5325–5333.
- (29) Yang, Y.-F.; Cederbaum, L. S. Bound states and symmetry breaking of the ring C_{20}^- anion. *J. Chem. Phys.* **2020**, *152*, 244307.
- (30) Brémond, E.; Pérez-Jiménez, A. J.; Adamo, C.; Sancho-García, J. C. sp-hybridized carbon allotrope molecular structures: an ongoing challenge for density-functional approximations. *J. Chem. Phys.* **2019**, *151*, 211104.
- (31) Baryshnikov, G. V.; Valiev, R. R.; Nasibullin, R. T.; Sundholm, D.; Kurten, T.; Ågren, H. Aromaticity of even-number cyclo[n]-carbons ($n = 6 - 100$). *J. Phys. Chem. A* **2020**, *124*, 10849–10855.
- (32) Heaton-Burgess, T.; Yang, W. Structural manifestation of the delocalization error of density functional approximations: C_{4N+2} rings and C_{20} bowl, cage, and ring isomers. *J. Chem. Phys.* **2010**, *132*, 234113.
- (33) Sonnentrucker, P.; York, B.; Hobbs, L. M.; Welty, D. E.; Friedman, S. D.; Dahlstrom, J.; Snow, T. P.; York, D. G. A modern census of the broadest diffuse interstellar bands. *Astrophys. J. Supp. Ser.* **2018**, *237*, 40.
- (34) Hobbs, L. M.; York, D. G.; Thorburn, J. A.; Snow, T. P.; Bishof, M.; Friedman, S. D.; McCall, B. J.; Oka, T.; Rachford, B.; Sonnentrucker, P.; et al. Studies of the diffuse interstellar bands. III. HD 183143. *Astrophys. J.* **2009**, *705*, 32–45.
- (35) Maier, J. P.; Lakin, N. M.; Walker, G. A. H.; Bohlender, D. A. Detection of C_3 in diffuse interstellar clouds. *Astrophys. J.* **2001**, *553*, 267–273.
- (36) McCall, B. J.; Hinkle, K. H.; Geballe, T. R.; Moriarty-Schieven, G. H.; Evans, N. J., II; Kawaguchi, K.; Takano, S.; Smith, V. V.; Oka, T. Observations of H_3^+ in the diffuse interstellar medium. *Astrophys. J.* **2002**, *567*, 391–406.